One-dimensional electronic states in Ga_2Se_3 on Si(001):As

T. C. Lovejoy,[1,*] E. N. Yitamben,[1] T. Ohta,[2,†] S. C. Fain, Jr.,[1,‡] F. S. Ohuchi,[3] and M. A. Olmstead[1]
[1]*Department of Physics and Center for Nanotechnology, University of Washington, P.O. Box 351560, Seattle, Washington 98195, USA*
[2]*Advanced Light Source, Berkeley, California 94720, USA*
[3]*Department of Materials Science and Engineering, and Center for Nanotechnology, University of Washington, P.O. Box 352120, Seattle, Washington 98195, USA*
(Received 25 April 2010; published 15 June 2010)

Gallium selenide (Ga_2Se_3) is a III-VI chalcogenide material whose intrinsic cation vacancy ordering into one dimensional chains has been predicted to result in a one dimensional band at the valence-band maximum (VBM). The electronic structure of Ga_2Se_3 thin films on Si(001):As is studied with angle-resolved photoemission spectroscopy. The integrated density of states and the dispersion exhibit good agreement with that predicted by published density-functional theory results. Consistent with a one dimensional state, the electronic states at the VBM show no dispersion perpendicular to the vacancy chains. The Se-Ga bond length from extended x-ray absorption fine structure is 2.34 Å. Low-energy electron-diffraction results indicate that the surface is characterized by nanometer-scale (111) facets, consistent with previous scanning tunneling microscopy results.

DOI: 10.1103/PhysRevB.81.245313 PACS number(s): 73.21.Hb, 73.20.At, 71.55.Ht

I. INTRODUCTION

Intrinsic vacancy materials exhibit vacancy concentrations far in excess of the dilute limit. As a result, phenomena which depend on vacancy concentration are anomalously pronounced in these materials. Reduced kinetic barriers, leading to phase change applications in the technologically relevant GeSbTe,[1,2] and high radiation resistance due to the abundance of potential vacancy-interstitial recombination sites[3,4] are two examples. These materials also constitute an interesting testing ground for theoretical models of amorphous materials, as they are intermediate between amorphous and ordered crystals. Depending on whether the vacancies are considered intrinsic to the structure or structural defects, the same material can be called either a perfect crystal or highly defected/amorphous. For example, the anion sublattice in gallium selenide (Ga_2Se_3) exhibits long-range order in any crystal while the vacancies (33%) on the cation sublattice may be either randomly distributed or ordered.

Ga_2Se_3 is a III-VI chalcogenide semiconductor with intrinsic cation vacancies. Disregarding the vacancies, the structure is essentially the same as zinc-blende GaAs, but the increased cation-anion electron count mismatch, together with charge neutrality, force one third of the gallium lattice sites to be vacant. Various vacancy orderings are possible.[5,6] For known bulk orderings, every Ga has four Se neighbors, and there are two types of Se present in a 2 to 1 ratio: Se(3) with 3 Ga neighbors and Se(2) with 2 Ga neighbors. In the orthorhombic vacancy ordering, the vacancies self-assemble into one dimensional chains along the $[1\bar{1}0]$ direction.[5] This one dimensional vacancy structure has been predicted to result in a highly anisotropic electronic band structure with a one dimensional band at the valence-band maximum (VBM),[7,8] suggesting the possibility of one dimensional conduction.[9] However, we find no experimental study of the anisotropic conduction or electronic band structure of this material—this may be due to the difficulty of growing high-quality single crystals with the desired vacancy ordering.

In this paper, we use Si(001) as a template for the growth of very high-quality epitaxial thin films of Ga_2Se_3. Scanning tunneling microscopy (STM), low-energy electron diffraction (LEED), x-ray diffraction (XRD), and extended x-ray absorption fine structure (EXAFS) are used to characterize the atomic arrangement of the films. The electronic structure is studied with angle-resolved photoemission spectroscopy (ARPES), and the results are shown to exhibit good agreement with the results of published studies[7,8] using density-functional theory (DFT). Comparison with the DFT results allows an identification of the experimental bands by their atomic origin. We compare the electronic states with those of the closely related compound GaAs: the primary difference is the presence of lone-pair states at the VBM, which originate from Se with two vacancy neighbors, Se(2). Consistent with a one dimensional state, these states show dispersion along the rows, but no dispersion in the perpendicular direction. The vacancy rows also have a strong effect on the surface morphology. We observe streaks in the LEED pattern whose locations vary with incident-beam energy in a way characteristic of faceting. Together with the other structural characterization, this confirms the STM results[10] showing long (>20 nm) and narrow (<1 nm) (111) facets on the Ga_2Se_3 (001) surface.

II. GROWTH AND MEASUREMENT

The details of achieving epitaxial growth of Ga_2Se_3 on Si(001) by molecular-beam epitaxy are given elsewhere[10] and summarized briefly here. Si(001) substrates are prepared in ultrahigh vacuum (UHV) by long outgassing (~2 h 800 °C) followed by a series of short flashes (~10) up to ~1200 °C. The surface is then terminated with a single monolayer of As, and the As is thoroughly pumped out before a single Knudsen cell loaded with GaSe source material supplies an incident flux. Despite the stoichiometry of the source material, the substrate constrains the cubic Ga_2Se_3 to grow.[11] For photoemission and LEED experiments, the samples were grown at the Advanced Light Source Beamline

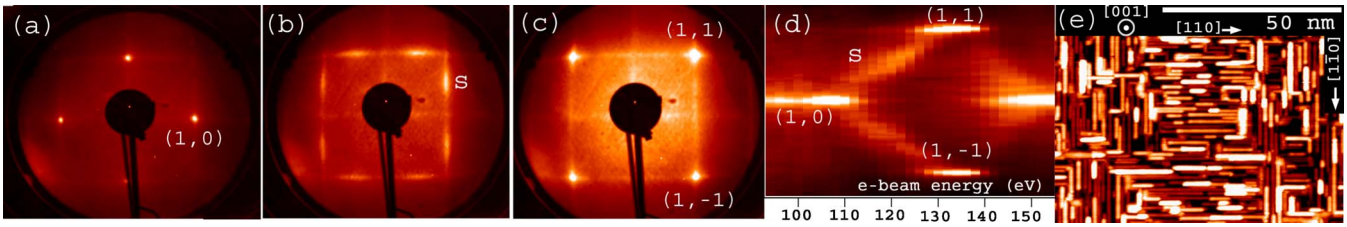

FIG. 1. (Color online) LEED pattern from Ga_2Se_3 film at (a) ~105 eV, (b) ~120 eV, and (c) ~135 eV. (d) Intensity as a function of beam energy (white=more intensity) for all the points along the line connecting the (1,1) and (1,−1) spots scaled to give a fixed separation between those two spots. (e) STM image showing two-domain wirelike structure of Ga_2Se_3 found by Ohta *et al.* (Ref. 10); horizontal scale bar (50 nm) and substrate orientation are indicated.

7 and transferred in UHV to the analysis chamber. Similar samples were grown in Seattle by the same method, checked for the characteristic LEED and STM signatures, and then transported in air for XRD in Seattle or EXAFS at the Advanced Photon Source Sector 20BM. The approximate film thicknesses for each film were between 2 and 5 nm.

For photoemission experiments, a hemispherical Scienta R4000 analyzer was used in conjunction with photons in the range from $80<h\nu<210$ eV with linear polarization inclined about 55° toward [001] from the [110] substrate direction. Binding energies are referenced to the VBM, which was 0.9 eV below the Fermi level measured on a metal clip on the sample holder. EXAFS data were taken and analyzed in the same way we reported previously for Mn-doped Ga_2Se_3.[12] XRD was measured with a Bruker D5000 with a copper $K\alpha$ source and a monochromator before a scintillator detector. LEED patterns were captured with a charge-coupled-device camera from a conventional apparatus using hemispherical acceleration grids and a phosphor screen.

III. RESULTS AND DISCUSSION

A. STM, XRD, and EXAFS

Structural characterization of the thin films was carried out with STM, XRD, and EXAFS. Typical STM results are shown in Fig. 1(e). Similar to those reported previously,[10] the surfaces are characterized by two domains of a wirelike morphology with "nanorods" tens of nanometers long with subnanometer width. Each substrate terrace is occupied almost exclusively by one orientation of nanowire, Si[110] or Si[1$\bar{1}$0], simultaneously making the substrate terraces easily recognizable in Fig. 1(e) and giving rise to the two domains. The lattice mismatch between bulk Si and Ga_2Se_3 is less than 0.1%, so, the zinc-blende (002) reflection, which is forbidden in silicon but allowed in Ga_2Se_3, was measured with XRD. Using a conventional θ-2θ scan, this reflection was found at $2\theta=32.92°$, corresponding to a cubic lattice constant of 5.436 Å or $0.1\pm0.02\%$ larger than Si (5.430 Å). The (002) peak is not observed on a region of the same substrate that was covered by a mask during growth.

The films take the Ga_2Se_3 phase, though subtle differences from bulk Ga_2Se_3 can be observed. In addition to the XRD characterization, the element-specific Se EXAFS data can be used to identify the Ga_2Se_3 phase. We observe a Se-first-neighbor bond length of 2.34 Å about 2% smaller than our measured value for a powdered Ga_2Se_3 reference sample (2.40 Å). The only other stable compound, layered GaSe, has a much larger bond length of 2.46 Å.[13] Due to the intrinsic vacancies in the Ga_2Se_3 structure in the bulk, it is expected that the Se-Ga bond length should be somewhat different than the 2.35 Å expected if all the atoms occupied their ideal zinc-blende positions. Structural relaxation with DFT predicts that the equilibrium Se-Ga bond length should be 5% larger than this.[7] The bond length in the thin film is closer to 2.35 Å than the relaxed bulk value, indicating the silicon likely constrains the thin-film atomic positions to lie closer to their ideal zinc-blende positions.

B. LEED

Ga_2Se_3 films exhibit a characteristic LEED pattern, shown in Fig. 1. Primary spots, indistinguishable from those expected for an unreconstructed Si surface, are present at all beam energies. As the incident energy is changed, relatively weak horizontal (vertical) streaks are observed to move horizontally (vertically) from spot to spot. Figure 1 shows a single LEED pattern at three incident-beam energies [Figs. 1(a)–1(c)]. When the spots are dim, as in Fig. 1(b), the streaks are clearly visible. The center of intensity for the streaks moves with changing beam energy. This is most clearly seen in Fig. 1(d), which shows the intensity of the line [scaled to give constant (1,1)-(1,−1) spacing] on the LEED screen connecting the (1,1) and (1,−1) spots as function of beam energy. The intensity (whiteness) along a horizontal line in Fig. 1(d) gives an $I(V)$ curve for a single k point. For example, a horizontal line through the middle of Fig. 1(d) gives an $I(V)$ curve for the (1,0) reflection. The streak feature is labeled "s" in Figs. 1(b) and 1(d). In Fig. 1(d) the center of intensity for the streak feature moves continuously from the (1,0) spot to the (1,1) spot with increasing beam energy. This motion is the same as that expected for (111) facets.[14]

We propose that the streak features are the diffraction pattern from the nanofacets of (111) Se sheets, supporting the model[10] that the intrinsic vacancies of Ga_2Se_3 take the orthorhombic vacancy ordering, with vacancy rows along Si[110] or [1$\bar{1}$0], and give rise to nanometer scale (111) sheets/facets. The center of intensity for the LEED streak features moves with beam energy as expected for (111) facets. From STM the facets are on the order of 1 nm tall by 30 nm wide. This narrow and long facet shape is responsible for the tall and skinny shape of the streak feature in the LEED pattern, consistent with the reported interpretation of STM images.

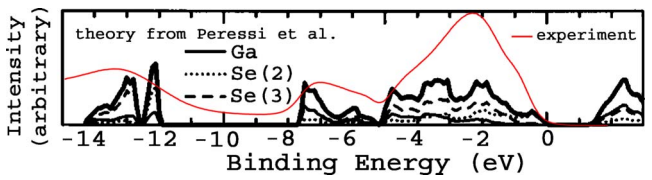

FIG. 2. (Color online) Integrated density of electronic states measured with ARPES (thin red) and total density of states plus breakdown by atomic species predicted by Peressi *et al.* using density-functional theory with LDA (thick black reproduced with permission from Ref. 7).

C. ARPES

The integrated density of electronic states determined by ARPES for the Ga_2Se_3 films exhibits good agreement with previously published DFT results[7] based on the local-density approximation (LDA), see Fig. 2. The integrated density of states was measured by integrating the photoemission intensity for $80<h\nu<210$ and over a 30° angular window along k_x, equivalent to integrating over ~3 Brillouin zones (BZs). Figure 2 also shows the DFT:LDA result for the total density of states from Peressi *et al.*[7] Both show three distinct envelopes of bands: one from 0 to −5 eV, a second from −5 to −8 eV, a ~4 eV "ionicity gap" with no bands, and then a final envelope from −12 to −14 eV. For both the experiment and theory, the total of the bandwidth above the ionicity gap is about 8 eV.

Before discussing the angle-resolved PES results, it is necessary to understand how the vacancy rows along Si[110] or Si[1$\bar{1}$0] affect the BZ. Following Peressi *et al.*, we use a right rectangular prism BZ arising from the orthorhombic supercell with two Ga_2Se_3 formula units. Due to the vacancy ordering along Si[110] (Si[1$\bar{1}$0]), the unit cell is three times longer along Si[1$\bar{1}$0] (Si[110]) than Si[110] (Si[1$\bar{1}$0]). Due to coupling between the vacancies within a given vacancy line, we expect little dispersion perpendicular to the vacancy line (ΓY), but a large dispersion parallel to it (ΓX). Since we have a two domain surface in the experiment, we expect to see a superposition of the dispersion along ΓY and ΓX as k_x is varied. The dispersion along k_z (ΓZ) will not be a superposition of dispersions because the two domains of in-plane vacancy ordering have the same structure along z.

The states at the VBM show little dispersion in ARPES while states lower in energy show clear dispersion. Figure 3(a) shows the normal-emission valence-band spectra along ΓZ for a series of values of k_z incremented by ~0.04 Å^{-1}. The data was collected in an angle-resolved window with constant steps in $h\nu$ and then converted to k_xk_z space according the scheme described in Ref. 15. The inner potential, $V_0=E_0-e\Phi$, is adjusted to put the observed symmetry point in the band dispersion at the Γ point expected at $k_z=7.0$ Å^{-1}. We use $e\Phi=4.5$ eV and $E_0=-7$ eV. A solid black vertical line marks the maximum binding energy of a shoulder at the VBM at Γ ($k_z=7.0$ Å^{-1}). The minimum binding energy of this shoulder occurs about 250 meV lower at the Z point ($k_z=5.8$ Å^{-1}). Over the same range of k_z, the maximum of the feature labeled "A" disperses by about 1.5 eV. Figure 3(b) shows the dispersion of the bands from the Γ point with k_x. The spectra at the BZ boundary points X and Y, which would be in perpendicular directions for a single domain sample, are shown in black (refer to the labels on the right of Fig. 3). Again, a black vertical line marks the position of a shoulder defining the VBM at Γ. We can resolve no dispersion in the location of this shoulder from the Γ point with k_x. However, the maximum of intensity of the VB exhibits a clear dispersion over the same range. As k_x changes, careful inspection reveals the feature labeled A in Fig. 3 splits into two components: one exhibits a dispersion of only ~250 meV while the other moves by about 1.5 eV. This is

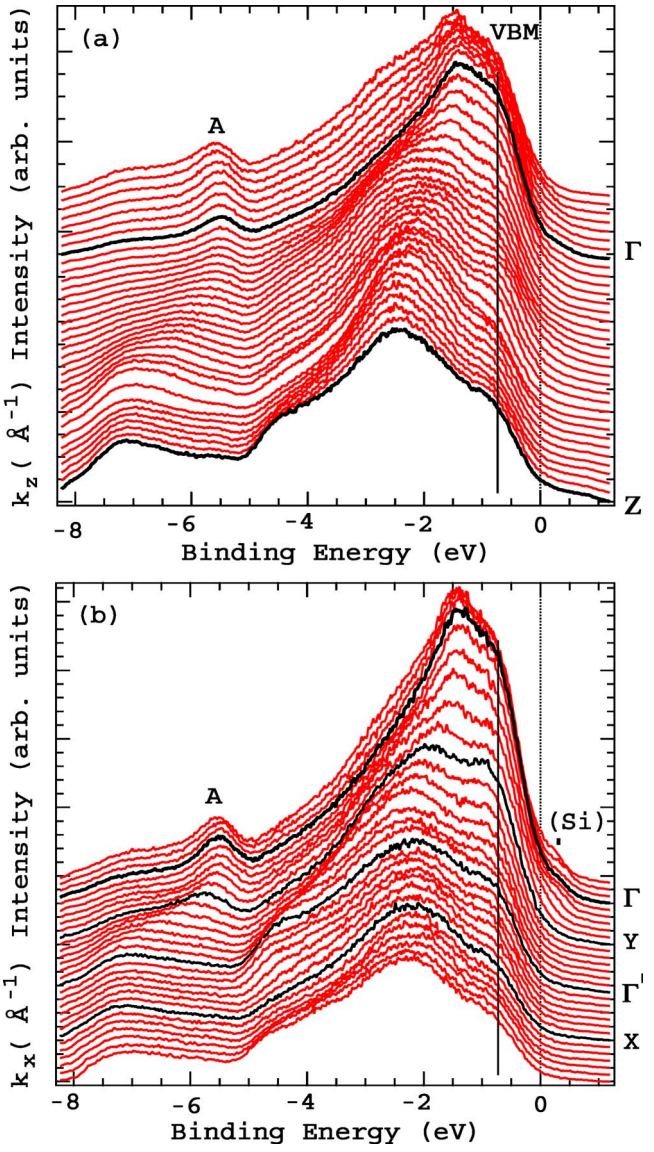

FIG. 3. (Color online) (a) Normal-emission valence-band spectra from ARPES. Spectra with increasing k_z (0.043 Å^{-1} increment) are offset to separate them. Black bold spectra are at Γ ($k_z\sim7.0$ Å^{-1}) and Z ($k_z\sim5.8$ Å^{-1}). See labels at right. (b) ARPES spectra from Γ along k_x (0.080 Å^{-1} increment). The black spectra are at Γ, Y (the BZ boundary along ΓY), Γ′ (a Γ point along ΓY), and X (the BZ boundary along ΓX, which is also another Y point along ΓY). A shoulder at the valence-band maximum shows little dispersion with k_z and is emphasized with a vertical black line—it exhibits no dispersion along k_x.

manifested in the data by the widening of A band by ~1.5 eV with increasing k_x. A "foot" in the density of states at Γ is labeled "Si." This comes from the VBM of the underlying silicon.

The agreement between the DFT:LDA result and the experimental result, both in the total density of states and in the calculated dispersion, is good. Furthermore, by correlating our ARPES results with the DFT calculations we can identify a one dimensional band at the valence-band maximum originating from the "dangling bond" *p* states of the Se(2). The top ~1 eV of the valence band is dominated by states from Se(2). Peressi *et al.* describe the VBM state in Ga_2Se_3 as an atomiclike *p* state oriented along the cubic $[1\bar{1}0]$ axis. This state shows a small dispersion along ΓZ, no dispersion along ΓY, but a large dispersion along ΓX in the calculated dispersion relations.[7,8] This is consistent with the behavior observed in our experimental data. The dispersion of the VBM along ΓZ [see Fig. 3(a)] is only about 250 meV, which agrees quantitatively with the prediction of Peressi *et al.* The ΓY/ΓX case is more complicated in the experiment due to the overlapping contributions from the two domains, but from Γ along k_x (ΓY/ΓX) the shoulder at the VBM shows no dispersion, consistent with the prediction along ΓY, see Fig. 3(b). The situation is more clear for the band labeled A, which stands out from the nearby bands and shows a similar trend as the VBM in the predicted dispersion relations. Along ΓZ, A disperses about 1.5 eV, which agrees with the predicted result to within the experimental width of the band. From Γ along k_x, A is observed to split into two bands with one band showing much more dispersion than the other. We can easily imagine this as a superposition of the same band dispersing along ΓX while remaining fairly flat along ΓY, see Fig. 3(b).

Comparison with DFT results also allows an assignment of the states below the VBM by atomic origin. Below the Se(2), *p* states at the VBM, there are *p* states of Se(3). Intuitively, comparing a given state of Se(2) to the same state in Se(3), the latter will be more bound because electrons of Se(3) are participating in additional bonding and therefore participating less in core screening. This is confirmed by the calculations, which find the "center of energy" for the Se(3) *p* states below that for Se(2) *p* states. The envelope of bands between 0 and −8 eV comes from Se *p* states, and both *s* and *p* states of Ga, with the *s* states near the lower edge. Below the ionicity gap, the calculations show two sharp peaks from Se(2) (shallower) and Se(3) (deeper) *s* states.[7] In the experimental spectrum, these states appear as a single broad peak with no separation even in the angle-resolved data (not shown). This could indicate that the distinction between the *s* states is not as sharp as predicted.

While DFT can produce accurate predictions for both the total density of states and band dispersions, calculations based on the virtual-crystal approximation (VCA) do not produce accurate results even for the total density of states. Guizetti *et al.*[16] computed the electronic density of states for Ga_2Se_3. They used the virtual-crystal empirical pseudopotential method to approximate a random vacancy arrangement by averaging the potentials from the isoelectronic compounds GaAs and ZnSe, and occupying the cation sites of the zinc-blende lattice with "atoms" whose potential was 2/3 that of the Ga-Zn average cation. The bandwidth predicted by this method is less than 5 eV, which is significantly less than the experimental or DFT result of 8 eV. The primary cause of the disagreement with the VCA may be that it does not respect the difference between Se(3) and Se(2).

It is interesting to compare experimental densities of states for Ga_2Se_3 with the other "isoelectronic" compounds such as GaAs. Isoelectronic means that both compounds have eight valence electrons per cation-anion pair if you consider the appropriate pair: Ga-As vs 2/3 Ga-Se. The width of the bands above the ionicity gap for GaAs is about 7 eV.[15] If one subtracts the 1 eV at the VBM from Se(2) *p* states, this is comparable to the bandwidth of Ga_2Se_3 (~8 eV). In the experimental data, the ionicity gap in GaAs is comparable to that in Ga_2Se_3 at about 4 eV but the density of states does not go completely to zero in this region (the band tails stretch into the gap). The ionicity gap predicted for Ga_2Se_3 is somewhat larger than that for GaAs,[7] which makes intuitive sense because the electronegativities of the cation and anion differ by a larger value. In the dispersion relations, Ga_2Se_3 has a local maximum 5 eV below the VBM at Γ. This is the band labeled A in Fig. 3. GaAs has no local maximum at Γ below the VBM. This "new state" may be considered to originate from zone folding due to the larger unit cell of Ga_2Se_3 relative to GaAs.

IV. CONCLUSION

In conclusion, high-quality Ga_2Se_3 films have been grown on Si(001):As. Streaks in the LEED pattern are due to nanoscale (111) facets, which supports the intrinsic vacancy ordering model.[10] The electronic structure is studied with ARPES, and the agreement with the predictions from calculations based on DFT is good. On the other hand, the agreement with calculations using the virtual-crystal approximation is poor. The DFT calculations predict a one dimensional state at the valence-band maximum due to intrinsic vacancy rows in the Ga_2Se_3 structure. Consistent with a one dimensional state, the VBM states show dispersion along k_z, but not k_x, in the measured dispersion relations. Compared to GaAs, the bandwidth of Ga_2Se_3 is about 1 eV larger, and there is a new local maximum at Γ 5 eV below the VBM arising from zone folding due to the larger supercell imposed by the vacancy ordering.

ACKNOWLEDGMENTS

Work was supported in Seattle by the NSF (Grant Nos. DMR-0605601 and DMR-0710641), and at the ALS by the DOE under Contract No. DE-AC02-05CH11231. T.C.L. acknowledges support from the IGERT program, NSF/NCI under Grant No. DGE 0504573 through the Center for Nanotechnology at the UW, and E.N.Y. acknowledges support from the IBM Corporation. Use of the Advanced Photon Source is supported by the DOE under Contract No. DE-AC02-06CH11357, and the authors acknowledge S. M. Heald for assistance with the EXAFS measurements.

*tlovejoy@uw.edu
†Present address: Sandia National Laboratories, Albuquerque, NM 87185, USA.
‡Deceased.

[1] M. Wuttig, D. Luesebrink, D. Wamwangi, W. Welnic, M. Gillessen, and R. Dronskowski, Nature Mater. **6**, 122 (2007).
[2] Z. Sun, J. Zhou, and R. Ahuja, Phys. Rev. Lett. **96**, 055507 (2006).
[3] K. V. Savchenko, Tech. Phys. Lett. **34**, 964 (2008).
[4] X.-M. Bai, A. F. Voter, R. G. Hoagland, M. Nastasi, and B. P. Uberuaga, Science **327**, 1631 (2010).
[5] E. Finkman, J. Tauc, R. Kershaw, and A. Wold, Phys. Rev. B **11**, 3785 (1975).
[6] D. Lübbers and V. Leute, J. Solid State Chem. **43**, 339 (1982).
[7] M. Peressi and A. Baldereschi, J. Appl. Phys. **83**, 3092 (1998).
[8] T. Nakayama and M. Ishikawa, J. Phys. Soc. Jpn. **66**, 3887 (1997).
[9] M. Ishikawa and T. Nakayama, Phys. Status Solidi B **229**, 301 (2002).
[10] T. Ohta, D. A. Schmidt, S. Meng, A. Klust, A. Bostwick, Q. Yu, M. A. Olmstead, and F. S. Ohuchi, Phys. Rev. Lett. **94**, 116102 (2005).
[11] T. Ohta, Ph.D. thesis, University of Washington, 2004.
[12] T. C. Lovejoy, E. N. Yitamben, S. M. Heald, F. S. Ohuchi, and M. A. Olmstead, Appl. Phys. Lett. **95**, 241907 (2009).
[13] S. Takatani, A. Nakano, K. Ogata, and T. Kikawa, Jpn. J. Appl. Phys., Part 2 **31**, L458 (1992).
[14] G. Ertl and J. Kuppers, *Low Energy Electrons and Surface Chemistry* (VCH, Florida, 1985).
[15] T. C. Chiang, J. A. Knapp, M. Aono, and D. E. Eastman, Phys. Rev. B **21**, 3513 (1980).
[16] G. Guizzetti, F. Meloni, and A. Baldereschi, Proceedings of the 15th International Conference on the Physics of Semiconductors, Kyoto, 1980 [J. Phys. Soc. Jpn. **49A**, 93 (1980)].